

TIME-DEPENDENT SIMULATIONS OF FILAMENT PROPAGATION IN PHOTOCONDUCTING SWITCHES

P. W. Rambo , W. S. Lawson,
*University of California, Lawrence Livermore National Laboratory**
P. O. Box 808, Livermore, CA 94551
C. D. Capps and R. A. Falk
Boeing Defense & Space Group
P. O. Box 3999, Seattle, WA 98124

ABSTRACT

We present a model for investigating filamentary structures observed in laser-triggered photoswitches. Our model simulates electrons and holes in two-dimensional cylindrical (r - z) geometry, with realistic electron and hole mobilities and field dependent impact ionization. Because of the large range of spatial and temporal scales to be resolved, we are using an explicit approach with fast, direct solution of the field equation. A flux limiting scheme is employed to avoid the time-step constraint due to the short time for resistive relaxation in the high density filament. Self-consistent filament propagation with speeds greater than the carrier drift velocity are observed in agreement with experiments.

I. INTRODUCTION

Laser-triggered solid-state switches operating at high fields have promising applications to fast pulse-power technology, to microwave generation, and may play an important role in impulse radar. Experiments with semi-insulating GaAs switches have shown exceptionally fast low-jitter operation in the high-gain regime, where the laser trigger energy is small compared to the switched electrical energy; see e.g. [1]. Connected with this efficient high-gain operation is the experimental observation of filamentary structures, which are suspected of carrying the bulk of the device current [2]. An understanding and characterization of these filaments is important for improving device performance and lifetime, and is the primary goal of our simulations.

Our model simulates electrons and holes in two-dimensional cylindrical (r - z) geometry. The continuity equation for each species s , with density n_s , is advanced in time with the particle flux expressed through a drift-diffusion type relation:

$$\frac{\partial n_s}{\partial t} = -\nabla \cdot (n_s \mathbf{u}_s) + \sum_{s'} \alpha_{s'} |u_{s'}| n_{s'}, \quad \mathbf{u}_s \equiv \frac{q_s}{e} \mu_s \mathbf{E}$$

Realistic coefficients for mobility μ_s and impact ionization α_s are included, both non-linearly dependent on the electric field. For the time and space scales of interest, both diffusion and recombination are unimportant, but could be easily included. In fact, the physical diffusion would be small relative to numerical diffusion. The electrostatic field is found from the Poisson equation (in CGS units),

$$\nabla^2 \Phi = -\frac{4\pi}{\epsilon} \sum_s q_s n_s, \quad \mathbf{E} = -\nabla \Phi$$

where ϵ is the crystal dielectric (assumed to be a constant), and the charge of a species is q_s ($-e$ and $+e$ for electrons and holes respectively).

Our strategy for numerical solution of this model is determined by the necessary time and space scales that must be resolved. Experimentally, these filaments are observed to have a radius on the order of tens of microns, thus we anticipate a typical cell size $\Delta r \approx \Delta z < 1 \mu\text{m}$. The switches are typically one to several millimeters in dimension, hence our system sizes will be many hundreds of zones on a side and

total number of grid cells $N_g \approx 10^5 - 10^6$. The relevant time scale to be resolved is the ionization time, $\Delta t < (u\alpha)^{-1} \approx 0.5$ ps. Switching times are of the order of 100 ps - 1 ns, so we can anticipate several thousand cycles necessary for a simulation.

II. NUMERICAL IMPLEMENTATION

Apart from accuracy, ie. properly resolving the phenomena of interest, there are stability restrictions on the time step, determined by the choice of numerical algorithms. The Courant limit on the continuity equation requires that the flow not transit a cell in less than one time step (similar arguments would lead to a time step restriction for explicit diffusion). For the spatial zoning typically employed in these simulations, however, neither of these conditions limits the time step beyond what is required for resolving the phenomena of interest. A more limiting constraint is due to the resistive relaxation time. A region of space charge tries to relax under the action of its self-consistent electrostatic field; if the time step is too large, the motion over-compensates generating an oppositely directed field of larger magnitude. The stability requirement for explicit differencing is that the resistive decay time be resolved,

$$\Delta t < \tau_r \quad , \quad \tau_r \equiv \frac{\epsilon}{4\pi e \sum_s n_s \mu_s}$$

For intrinsic GaAs at 300 K ($\mu \approx 5.3 \times 10^3$ cm²/V-s), the resistive decay time is approximately $\tau_r \approx (1300 \text{ s/cm}^3)/n_e$. Because of nonlinear mobilities, $\Delta t > \tau_r$ may be acceptable due to nonlinear saturation of the unstable oscillations. However, in the high density, low-field region of the filament this limit can be a serious constraint. Typical carrier densities in the filament are found to be $n \approx 10^{17} - 10^{18}$ cm⁻³, and so the resistive decay time is very small, $\tau_r < 10$ fs.

Typical semiconductor device simulation is concerned with steady state behavior and solution schemes use implicit methods, where all the terms on the right-hand side of the continuity equation are written at the advanced time. This requires the solution of large block matrix systems, which are iterated due to non-linearities in the equations. These methods are robust and efficient at finding final steady states, but excessively costly for our application. An alternative is to treat only the most troublesome term by using the advanced electric field to define the drift velocity; substituting into the Poisson equation determines the field equation for a non-iterative scheme. However, this non-separable field equation still precludes the use of very efficient rapid-elliptic-solvers, which are the preferred solution method because of the large system size and necessary number of cycles.

We have implemented a *flux limiting* scheme which still allows use of a direct, rapid solver for the Poisson equation. The drift term is defined by limiting the velocity compared to a simple explicit definition,

$$n_s^{n+1} = n'_s - \Delta t \nabla \cdot \left(n'_s \frac{q_s}{e} \frac{\mu_s^n \mathbf{E}^n}{(1 + \Delta t / \tau_r)} \right), \quad n'_s = n_s^n + \Delta t \sum_s \alpha_s^n \left| u_s^n \right| n_s^n$$

where superscripts denote time level and the primed density on the right hand side includes other terms advanced explicitly in time. In regions where the resistive decay time is well resolved (low density, low mobility), $\Delta t \ll \tau_r$, the flux takes on its usual value. In regions where $\Delta t \gg \tau_r$, (high density, high mobility) this flux limiting ensures that only enough density moves to shield out electric field fluctuations.

Currently, spatial differencing of the transport is fully upwind; with the diffusion neglected, this is equivalent to Scharfetter-Gummel [3] differencing in the (appropriate) high field limit. The problem domain is restricted to be "rectangular", ie. $0 < z < Z_{max}$ and $0 < r < R_{max}$. The zoning is logical rectilinear, but can be variable in space, specified at problem set up. We have implemented two choices for the field solution, a fast Fourier transform method (FFT) and a cyclic reduction (CR) package. Although restricted

to uniform zoning in the z direction, the FFT package is substantially faster on vector machines like the CRAY Y-MP. The left and right boundaries for z are electrodes, and so defined to be equipotential surfaces. The system potential may be fixed or determined by an external circuit. At $r=0$, the radial electric field E_r must vanish in the absence of a line charge on axis; similarly $E_r=0$ at $r=R_{max}$ to approximate a transition to plane parallel equipotential surfaces.

III. REPRESENTATIVE RESULTS

To demonstrate the utility of our model, we present representative results from simulations of filament propagation. The system is $0 < z < z_{max} = 256 \mu\text{m}$, and $0 < r < R_{max} = 100 \mu\text{m}$. Zoning in the z -direction is constant, $\Delta z = 0.50 \mu\text{m}$; there are 51 radial zones, with $\Delta r = 0.50 \mu\text{m}$ at the axis and monotonically increasing to the radial boundary. This small system size and coarse zoning was picked to allow a calculation with small enough time step to avoid instability without flux limiting. Material parameters are typical for GaAs, except that the mobility model used here is monotonic to avoid complications from NDR and Gunn domain formation. A uniform background of electrons and holes representing the photo-generated carriers is initialized with a density of $n_0 = 1 \times 10^{14} \text{ cm}^{-3}$. To initiate the filament, a high density needle is initialized at the left hand side of the system, with radius $10 \mu\text{m}$, length $60 \mu\text{m}$, and density $1 \times 10^{17} \text{ cm}^{-3}$. The system is initially charge neutral, so that at time $t=0$, the electric field is uniform with $E_0 = 100 \text{ kV/cm}$ (negative z -direction); the system potential is fixed in time. In the first few picoseconds of the simulation, the electric field is excluded from the needle with a large enhancement developing at the tip, which eventually breaks down. The filament then propagates, with the density and tip shape determined self-consistently. A contour plot of electron density at $t=140 \text{ ps}$ (Fig. 1a) clearly shows the initial perturbation ($z < 60 \mu\text{m}$), a transition region ($60 \mu\text{m} < z < 80 \mu\text{m}$), and the propagating filament ($z > 80 \mu\text{m}$); contours of potential are shown in Fig. 1b. As the filament transits the device, the potential drop occurs over a smaller distance between filament head and anode increasing the field strength which leads to increasing filament radius and density. This qualitative effect of increasing

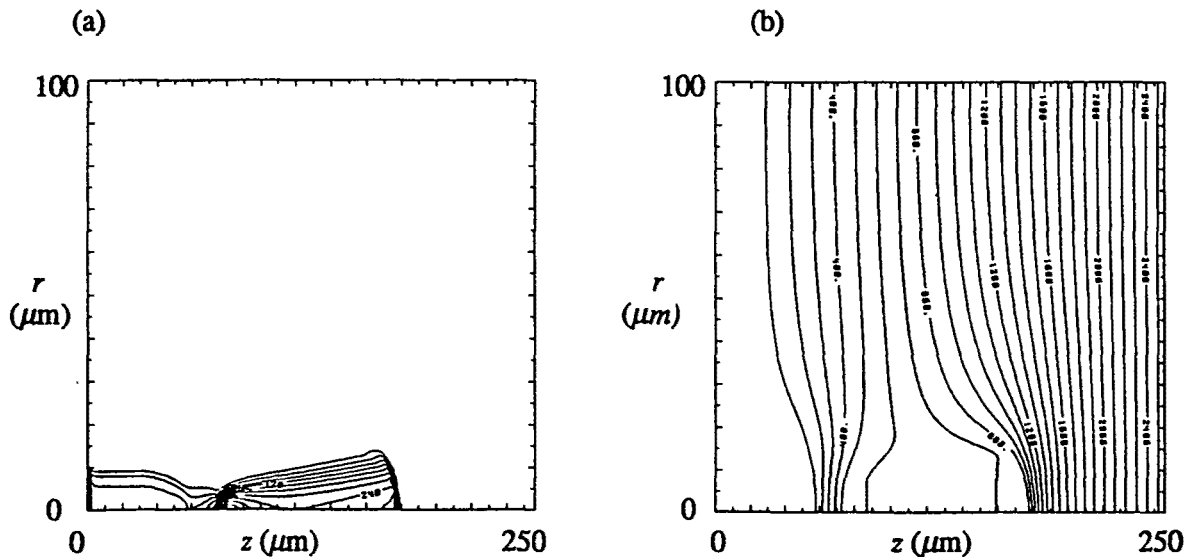


Fig. 1 Flux limited filament calculation at $t=140 \text{ ps}$, showing (a) contours of electron density, and (b) contours of electric potential; time step is $\Delta t = 5.0 \times 10^{-14} \text{ s}$.

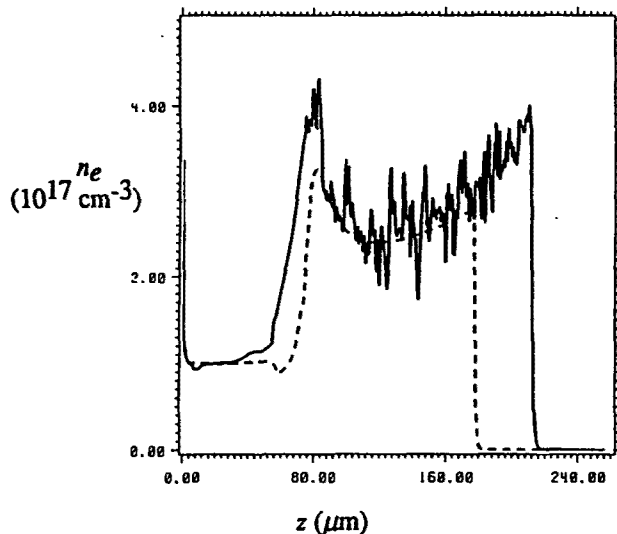


Fig. 2 Axial electron density $n_e(z)$ at time $t=140$ ps; solid line is without flux limiting, dashed is flux limited (identical to Fig. 1), $\Delta t=5.0 \times 10^{-14}$ s.

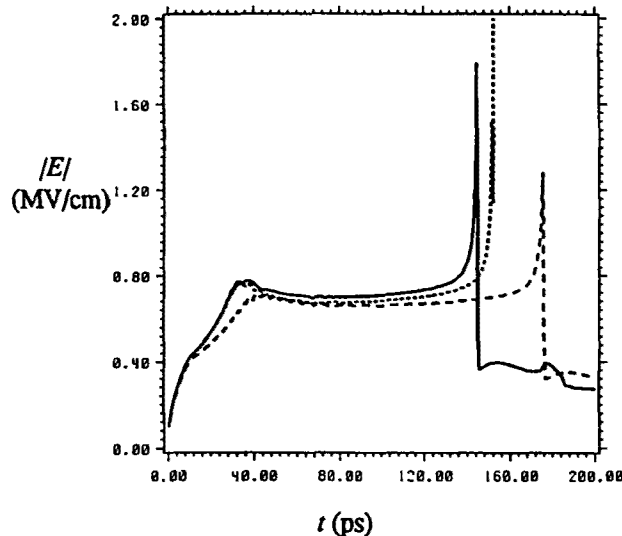


Fig. 3 Magnitude of electric field at filament head versus time: solid, $\Delta t=2.5 \times 10^{-15}$ (no flux limit); dashed (flux limited) and dotted (no flux limit), $\Delta t=5.0 \times 10^{-14}$ s.

radius is missing in previous filament simulations which mocked up the field enhancement in one dimensional calculations and picked the filament radius as a parameter [4].

This calculation was performed with flux limiting and a time step of $\Delta t=5.0 \times 10^{-14}$ s. An otherwise identical calculation but without flux limiting is compared in Fig. 2a, which shows the axial ($r=0$) profile of electron density n_e at time $t=140$ ps; unstable oscillations are obvious. The gross features of the two simulations are quite similar, except for a somewhat smaller propagation speed in the flux limited case. The calculation without flux limiting might be considered satisfactory, except that as the filament finally completes its transit across the system, instability terminates the calculation and prevents the subsequent determination of the switched current. A comparison of the previous two calculations with one using a time step $\Delta t=2.5 \times 10^{-15}$ s and no flux limiting is presented in Fig. 2b, which shows the magnitude of the electric field at the filament head versus time.

* This work was supported by the U. S. Department of Energy at Lawrence Livermore National Laboratory under Contract W-7405-Eng-48.

- [1] F. J. Zutavern et al., "Photoconductive Semiconductor Switch Experiments for Pulsed Power Applications," *IEEE Trans. on Electron Devices* ED-37, 2472 (1990).
- [2] J. C. Adams, R. A. Falk, C. D. Capps, and G. Bohnhoff-Hlavacek, "Characterization of Current Filamentation in GaAs Photoconductive Switches," *Proc. SPIE* 1873, 10 (1993).
- [3] D. L. Scharfetter and H. K. Gummel, "Large-Signal Analysis of a Silicon Read Diode Oscillator," *IEEE Trans. on Electron Devices* ED-16, 64 (1969).
- [4] C. D. Capps, R. A. Falk, and J. C. Adams, "Time-dependent model of an optically triggered GaAs switch," *J. Appl. Phys.* 74, 6645 (1993); D. W. Bailey, R. A. Dougal, J. L. Hudgins, "Streamer propagation model for high-gain photoconductive switching," *Proc. SPIE* 1873, 185 (1993).